CLINICAL AND EXPERIMENTAL
OPTOMETRY

INVITED REVIEW

Anterior ophthalmic imaging

Clin Exp Optom 2006; 89: 4: 205–214 DOI:10.1111/j.1444-0938.2006.00065.x

James S Wolffsohn BSc PhD
Rachael C Peterson BSc
School of Life and Health Sciences, Aston University, Birmingham, United Kingdom
E-mail: j.s.w.wolffsohn@aston.ac.uk

Submitted: 31 January 2006
Revised: 17 April 2006
Accepted for publication: 28 April 2006

Improvements in imaging chips and computer processing power have brought major advances in imaging of the anterior eye. Digitally captured images can be visualised immediately and can be stored and retrieved easily. Anterior ocular imaging techniques using slitlamp biomicroscopy, corneal topography, confocal microscopy, optical coherence tomography (OCT), ultrasonic biomicroscopy, computerised tomography (CT) and magnetic resonance imaging (MRI) are reviewed. Conventional photographic imaging can be used to quantify corneal topography, corneal thickness and transparency, anterior chamber depth and lateral angle and crystalline lens position, curvature, thickness and transparency. Additionally, the effects of tumours, foreign bodies and trauma can be localised, the corneal layers can be examined and the tear film thickness assessed.

Key words: anterior eye, imaging, photography, slitlamp biomicroscopy

'Imaging' can be defined as the visual representation of an object, usually in the form of an objective recording. The advent of photography in 1826 created the opportunity for an image to be captured for subsequent visualisation of a scene.[1] The potential of image capture was recognised by the medical community, which was encouraged to obtain accurate and permanent descriptions of anatomical features for reference or monitoring of disease. Since the achievement of the first human retinal photograph in 1886 by Jackman and Webster,[2] the ophthalmic community has embraced imaging technology in many forms to enhance its understanding and management of ocular disease.

FILM-BASED PHOTOGRAPHY

Rapid developments were made in film-based photography during the 20th Century. New emulsions reduced the exposure time necessary to capture an image; the original exposure time to capture the fundus was more than two minutes.[2] Colour photography was first achieved in 1861 by James C Maxwell,[3] with colour photographs of the fundus being described in 1929.[4] Developments in electricity and the availability of artificial light sources allowed Gullstrand to apply a slit-beam during ocular examinations to improve observations of anterior ocular structures and the lens.[5] Electric flash tubes were adapted for use in ophthalmic photography in 1946 by Harold Edgerton,[4] which greatly improved images of the fundus.

A traditional analogue camera is a basic device, exposing a piece of film through a lens and shutter. Photographic films are coated with crystals of a silver halide, usually silver bromide. The crystal atoms are electrically charged, with positively charged silver ions and negatively charged bromide ions. These are maintained in an evenly-spaced cubic grid by their electrical attraction. When the film is exposed to light energy, the photons of light release electrons from the bromide ions, which collect at defects in the crystal (sensitivity specks), which in turn attract an equal number of free silver ions. The silver atoms (black deposits) are amplified in

the processing stage by chemicals to create the negative image.[6]

Usually multiple images are recorded on one film and processing takes some time, interrupting the continuity of care of a patient, adding to administration of patient files and whether the images are of sufficient quality cannot be assessed immediately with the patient present. Polaroid film had the advantage of almost instant development but the image quality and durability were inferior to those of 35 mm colour transparencies.[6] The use of photography in optometric documentation was encouraged but the expense of the medium limited its use outside the Hospital Eye Service.[5]

DIGITAL IMAGING

In comparison to film-based photography, where the 'complexity' is in the design of the film and processing, a digital camera is more intricate, with the image processed electronically within the cameras. Few 'digital' photo-sensors are as large as a piece of 35 mm film, so camera lenses have to have a shorter focal length to achieve the same image size (typically 1.4 to 1.6 times).[6] Digital images can be viewed instantaneously on a monitor, enhanced or magnified and stored on a computer hard drive, disc or memory stick.[4]

There are several advantages of digital imaging.

1. Good quality of captured images

The voltage generated by the photons of light captured at each of the photosites (pixels) is assigned a numerical code in binary form, which contributes to the pattern used to recreate the image optically. This system is robust to electronic interference and transferring errors. The assigned code is measured in 'bits' (binary digits). The arrangement of pixels has been shown to be more regular than film based emulsion.[6]

2. Immediate visualisation of the captured image

As the processing of the captured photons is conducted within the camera, the images can be viewed almost instantaneously, allowing images to be retaken if unsatisfactory. Multiple images can be taken to optimise the magnification, illumination and camera position without incurring additional cost. The preferred images can be filed in electronic or printed form with the patient's notes without the need for subsequent image identification and additional filing. Additional non-optimal images can be deleted and the electronic storage space reused.

3. More efficient storage of the captured image

The digital format of the data, which code for the images, allows efficient archiving options and the ability to retrieve, reanalyse and display images of interest with considerable ease. Video-clips of dynamic presentations can be captured as well as static images. The technology improves rapid communication, not just between practitioners but also with patients, who benefit from more detailed and visual explanations of their conditions.[7]

In addition to documenting the appearance of the anterior eye, digital imaging can be used to assess the anterior chamber depth and angle (particularly useful in glaucoma), intraocular lens positioning and posterior subcapsular thickening (useful in cataract and presbyopia research) and to determine the central corneal thickness.[8–10] The latter has increased in importance, as its role in the measurement of intraocular pressure is better understood and with the development of laser refractive surgery.[11,12]

Generally, digital cameras have been more expensive than the film-based equivalent and there is a delay between pressing the capture button and the image being taken, making them less useful for static capture of fast moving objects. Digital image capture is usually associated with high resolution images, which take time to transfer from the light detection chip to the storage location, limiting the number of full images that can be captured and displayed each second. Transfer technology from the imaging chip to the storage site will need to improve to reduce the resulting jerky dynamic display, especially as imaging chip resolution increases.

Typically, digital cameras have one of three types of light detection chip. Charged couple devices (CCDs), like complementary metal-oxide semi-conductors (CMOS), consist of etched pixelated metal oxide semiconductors made from silicone, sensitive in the visible and near infrared spectrum. They convert light that falls onto them into electrons, sensing the level/amount of light rather than the colour. On CCDs, only the photon-to-electron conversion is conducted on the pixel areas, allowing the maximum amount of space to remain within each pixel for capturing light information. Therefore, they have a low signal-to-noise ratio. Both the photon-to-electron and electron-to-voltage conversions are conducted within a CMOS chip pixel area, together with digitisation of the signal, leaving less room for the light sensitive part of the sensor. Normally, a microlens is used to capture more light within the pixel area and bend it towards the light sensitive part of the pixel (the fill factor). CMOS chips have the advantage of being cheaper and less power hungry than CCDs, due to having fewer components, making them more reliable. Foveon imaging chips consist of three layers of CMOS imagers embedded in silicon, positioned to capture red, green and blue light as different wavelengths (and hence colour) of light are absorbed at different depths of silicon. Therefore each pixel can record full colour information on a single chip.[6]

Image quality

Most often, image quality is referred to in terms of resolution, which is the ability to distinguish the difference between two sequential points. Image resolution has different definitions depending on the method of image capture. For digital photography, resolution is defined as the number of pixels contained within an image of a certain size.[6] To resolve the presence of an object of interest, the pixel size needs to be at most half the size of that object as otherwise positioning across a pixel border may prevent visibility. The units of digital resolution are described in pixels per inch (ppi).[4] When considering 35 mm film, the resolution is known in terms of line pairs per mm (lp/mm). The most common type of camera

film can resolve between 40 and 65 lp/mm. It has been calculated that this number of lp/mm equates to the digital equivalent of approximately 4,000 × 6,500 ppi.[13] Therefore, a standard piece of 35 mm film, which is approximately 1.5 inches in diameter, will contain between 6,000 to 9,750 pixels horizontally. The height of the film is approximately one inch, which would equate to between 4,000 to 6,000 pixels vertically. Taking this range into account, the number of pixels required by a digital image to be comparable with the resolution of a standard analogue photograph is between 24 and 64 million pixels (also known as megapixels). Despite the lower resolution of digital images, improvements in digital technology have resulted in a sensitivity and specificity to detect retinal pathology comparable with analogue images and direct observation of patients by ophthalmologists.[9,10] The Diabetic Retinopathy Screening Committee concluded that fundus photography with 1,000 × 1,000 pixels is adequate to match the resolving power of the human eye over a 45 degree visual field but adjusted the requirement to 1,365 × 1,000 pixels to allow for the rectangular shape of digital camera image sensors.[14] Image quality is also dependent on the contrast of objects of interest, which can be enhanced by appropriate ambient and focal lighting, as well as techniques such as thresholding and edge detection algorithms.

Image storage

Two of the major considerations with digital imaging are the resolution needed to image objects of interest and the compression that can be used to minimise the space needed to store the image.[15] If photographs are to be used to detect pathology and monitor progression, and to protect against litigation, it is essential that the resolution is sufficient to allow all clinical features of interest to be detected and that this is not compromised by the image storage (Figure 1). However, the more space images occupy, the quicker storage space is used and database speed is slowed, compromising one of the major advantages of digital image capture. Smaller images also allow more efficient teleophthalmological screening.[16]

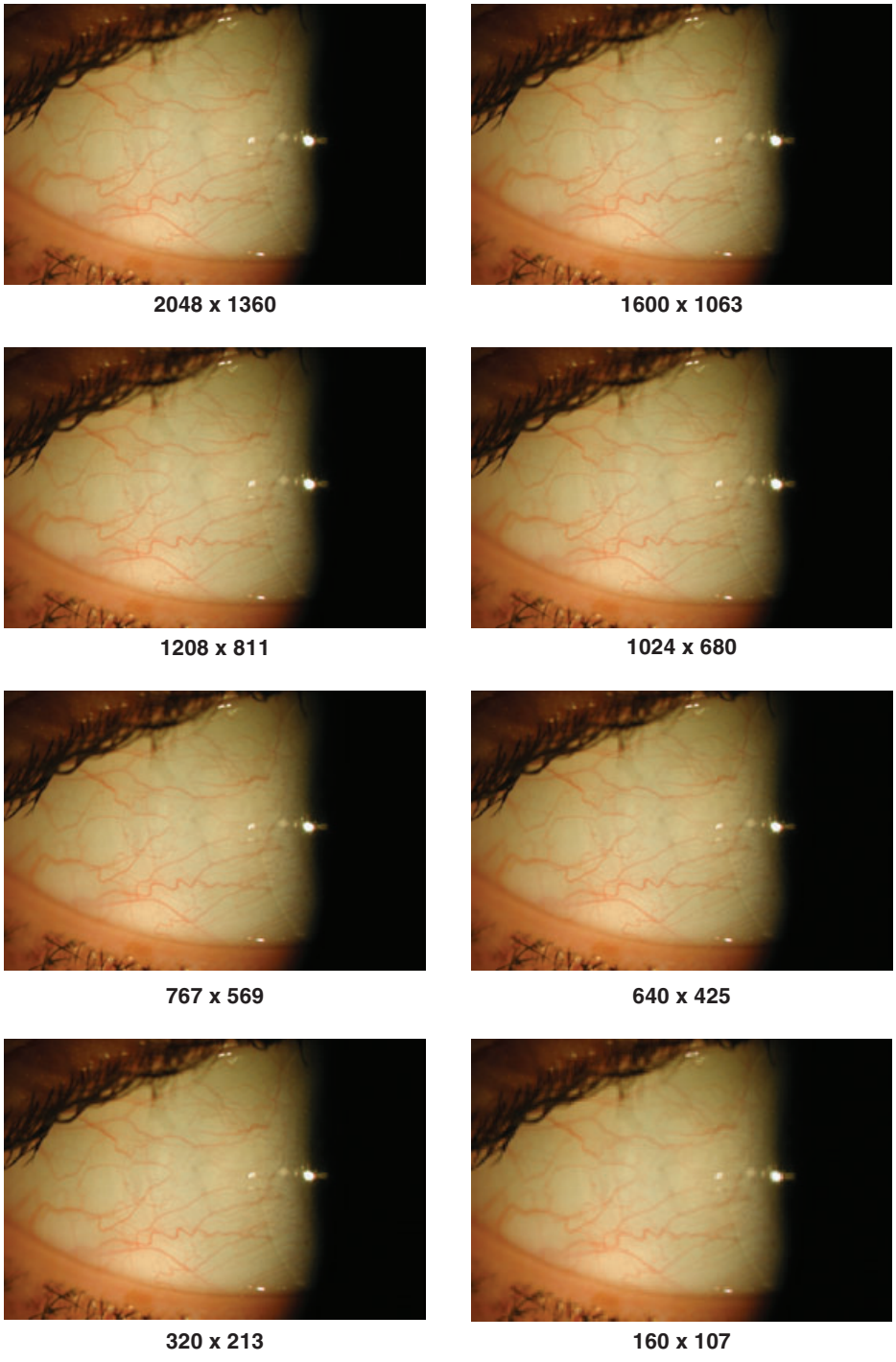

Figure 1. Images of the anterior eye with different pixel resolutions

Image compression is a technique that reduces file size by removing redundant information. In some compression methods the full information can be retrieved (termed 'lossless' formats such as TIFF) but in others, information is permanently

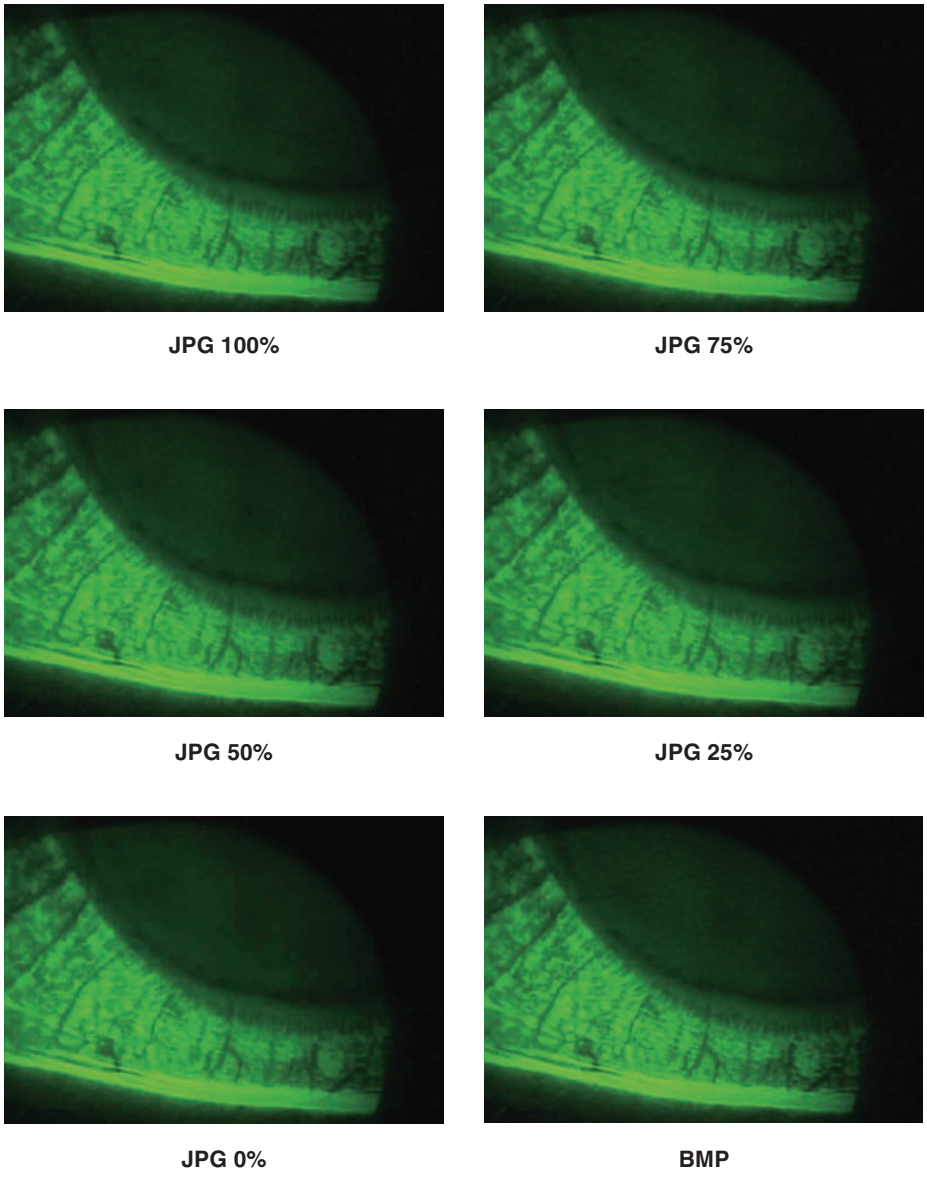

Figure 2. Images of the anterior eye compressed to different algorithm levels

deleted ('lossy' formats, such as JPEG).[4] Most digital imaging systems offer a selection of different file formats, with which to save images and movies (Figure 2). There are two types of graphic files, vectors and bitmaps. Vector files (such as Window Meta Files [*.wmf] and the Pict format used by Macintosh computers) split the image into shapes (such as lines and rectangles), describing their position within the image and their colour. The image is reconstructed from these shape instructions when reopened. As a result, the image size can be expanded or contracted without any effect on image quality but Vector files are not as suited to complex objects such as real images of an eye. The whole image of a bitmap file is divided into tiny squares (pixels) and the light intensity of the principal colours of each pixel is recorded. The result is a relatively large file and an image that cannot be enlarged without loss of resolution. The most commonly used bitmap format options are:

1. TIFF (tagged information file format): store all the raw data from the camera image in a standard lossless format.
2. JPEG (Joint Photographic Experts Group): a compressed format, resulting in the loss of some image integrity. JPEG compression attempts to eliminate redundant or unnecessary information in the form of frequencies not used by the human eye by using 'discrete cosine transforms' (lossy compression). Different compression levels can usually be selected. Previous studies on retinal imaging have suggested that up to 75 per cent quality JPEG compression can be applied to an image file without significant loss of subjectively assessed detail.[15,17,18]
3. BMP: Microsoft Windows native bitmap format. These are relatively large files and will reduce the original image quality to that of a medium quality (approximately) JPEG image.[19]
4. RAW: a more recent option allowing the captured data to be stored in raw form, before any procession has taken place. This results in a smaller image file than the TIFF format and the archived data are always available for reprocessing. Generally, cameras have different RAW data formats, so the image cannot be opened on other computer systems.

Slitlamp biomicroscopy allows a magnified view of the anterior eye and therefore the resolution required to distinguish a feature of interest will depend on the magnification. Theoretical calculation based on the smallest objects of interest in the anterior eye suggested a resolution of approximately 700 pixels horizontally for a magnification level of 20 times to resolve microcysts and punctate staining.[19]

Four cameras attached to the same slitlamp were used to capture images of the bulbar conjunctiva, palpebral conjunctiva and central corneal staining, which were assessed by subjective ranking of a range of images varying in resolution and compression.[19] Validated objective image analysis grading of the same images was also

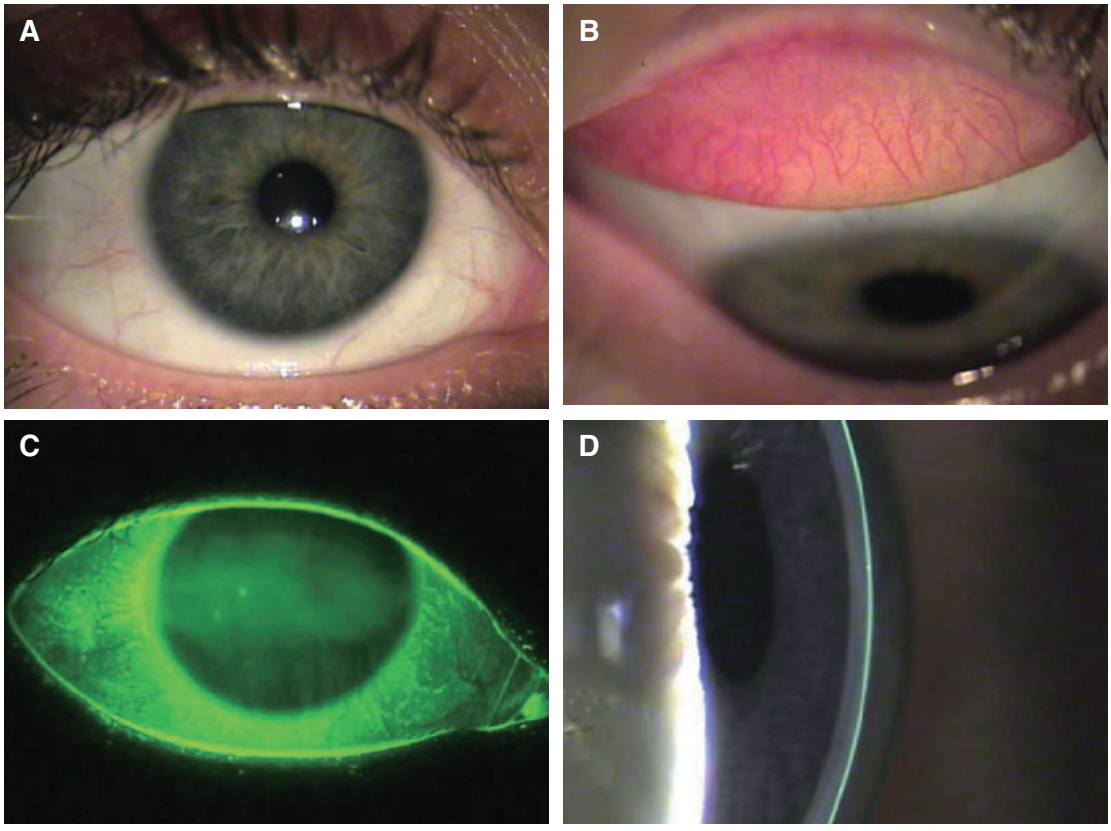

Figure 3. Digital slitlamp captures images of A: bulbar hyperaemia, B: palpebral hyperaemia, C: tear film with fluorescein instilled, D: corneal section

conducted.[20] Subjectively, images were not detectably degraded until they were reduced to 640 by 425 pixels resolution or 25 per cent quality JPEG compression. Despite the 'lossless' compression technique of BMP images, these were ranked to have visibly poorer quality than the original TIFF images. There was no significant difference in resolution or compression ranking between the camera models. It was also noted that if the resolution of the image was much greater than the monitor resolution on which the images were assessed, the subjective rating was worse due to the interpolation performed by the computer to fit the image into the available screen pixels. Objective grading was affected significantly, when the image size was reduced to 320×213 pixels resolution and was unaffected by image compression.[19]

ANTERIOR OCULAR IMAGING TECHNIQUES

Slitlamp biomicroscopy

The slitlamp biomicroscope is the most commonly used instrument in ophthalmic practice to observe the anterior eye, allowing manipulation of the enlargement and illumination of the observed image (Figure 3). Image capture can be achieved by inserting a beam splitter or mirror in the observation path before the eyepieces or by attaching a camera to an eyepiece. An additional external light source is usually required to compensate for the light lost by the beam-splitter, incomplete fill factor of CMOS imaging chips and the lower light sensitivity of the imaging chip compared to the human eye. As with retinal imaging, techniques such as green (red free) light for viewing blood vessels, can be used to enhance the captured image.[21] Image capture can allow automatic objective grading of the characteristics of the anterior eye, such as hyperaemia, staining,[20] corneal transparency,[22,23] lenticular opacification[24] and feature size and shape.[25] As with other digital imaging, the captured pictures can then be compressed and transmitted for teleophthalmic screening.[16]

Scheimpflug technique

The Scheimpflug principle images the anterior eye with a camera perpendicular to a slit-beam, creating an optical section of the cornea and lens (Figure 4). It has been used for the assessment of cataract,[26,27] crystalline lens shape changes with accommodation,[28] corneal haze,[29–31] corneal curvature and corneal thickness.[32]

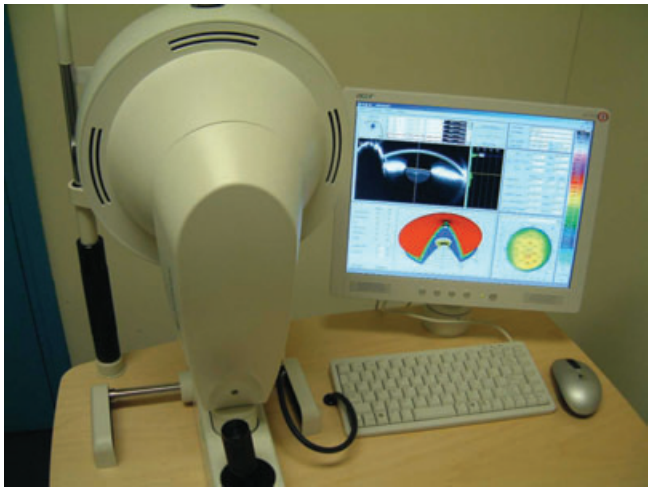

Figure 4. Scheimpflug device showing a captured image of the anterior eye

Figure 5. Corneal placido and raster topographer showing a contour map of the cornea

More recent instruments have been designed to rotate around the visual axis, capturing multiple images to create a three-dimensional image of the anterior chamber. Scheimpflug measures of central corneal thickness and anterior chamber depth have good repeatability compared to Orbscan topography, ultrasonography and magnetic resonance imaging (MRI).[33–35]

Corneal topography

Using the cornea as a convex mirror, measuring the size of the reflection of a light source of known dimensions at a set distance can be used to calculate the topography of the front surface of the cornea (Figure 5). Usually, multiple light concentric rings are reflected off the cornea (reflection system) and the image captured by a central camera. The image is transferred to a computer image capture board, with the position of the reflected rings analysed and displayed as colour-coded isobars of corneal radius or power. Alternatively, a slit beam of light can be passed across the cornea (projection system) and imaged multiple times at an offset angle (in a similar manner to Scheimpflug imaging) to quantify the curvature of both the front and back surfaces of the cornea, together with the corneal thickness (know as raster topography or posterior apical radius imaging).[36] The accuracy and reproducibility are similar to Placido-based systems (approximately four microns in the central cornea and seven microns in the periphery under optimal conditions) but the technique does not require an intact epithelial surface.[37] Due to the longer capture time for the multiple images, it is more dependent than Placido-based corneal topography on factors such as the patient's fixation and ability to keep the eye open.

Confocal microscopy

Conventional microscopes collect all the light reflected back from an object, with blurred light from out of the focal plane resulting in optical noise, limiting the resolution of the technique. Therefore, objects of interest need to be thinly sliced and the technique is not applicable to *in vivo* anatomical section imaging. In confocal microscopy, the pinhole source of light (such as a laser beam) and its conjugate pinhole detector limit the out-of-focus signal that is collected (Figure 6). However, the field of view is small and scanning is used to create a larger image. The scanning is usually achieved by rotating discs with multiple optically conjugate source-detector pinholes. Confocal microscopy has a resolution of approximately one micron and a maximal imaging depth of about 2.7 mm, which allows it to image cells of the corneal epithelium, the epithelial nerve plexus, different parts of the stroma and the endothelium.[22] *In vivo* corneal confocal microscopy can be used to make direct observations on living tissue, avoiding the shrinkage and distortion associated with conventional processing and sectioning for light microscopy.[38] Confocal microscopy has improved understanding of the function of each of the corneal layers and their spatial location[39] and has been extensively used to evaluate the progression and healing following inflammation or infection over time.[40–42] Confocal microscopy through focusing (CMTF) has been used in photorefractive surgery to assess corneal thickness, photoablation depth and corneal light scatter.[43] However, confocal microscopy is limited to the assessment of a small area of the central cornea, which reduces its efficacy.

Optical coherence tomography

Optical coherence tomography (OCT) is a non-invasive optical method allowing cross sectional imaging at a resolution of six to 25 µm (Figure 7). Ultrahigh resolution OCT with a spatial resolution of 1.3 µm can now be achieved.[44] This allows

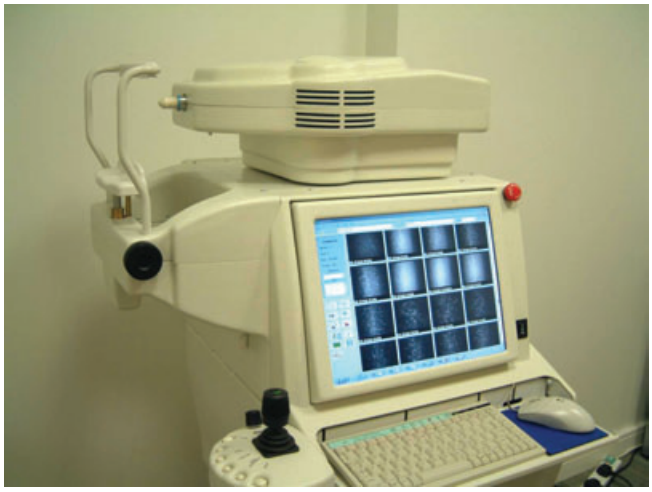

Figure 6. Confocal microscope showing captured images of the epithelium, stroma and endothelium

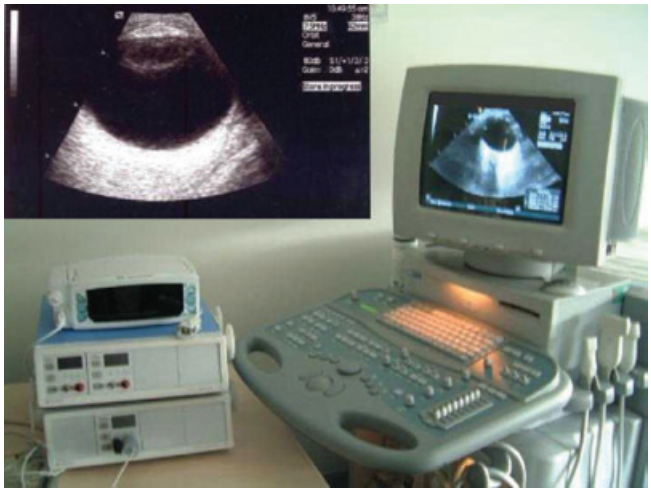

Figure 7. Optical coherence tomographer showing a captured image of the anterior eye

imaging of the corneal layers and measurement of their thicknesses. The technique works by splitting a light source into a reference and measurement beam. Light from the measurement beam is reflected from the ocular structures and interacts with the reference light reflected from the reference mirror causing interference. Coherent (positive) interference is measured by an interferometer, to allow an image of the reflected light from the ocular structures to be built up.[45] In imaging of the anterior eye, it has been used to measure tear film thickness[45–47] and to examine the cornea and limbus,[48] intraocular lens parameters, anterior chamber depth and the irido-corneal angle (even behind an opaque cornea).[49] OCT can penetrate the human sclera *in vivo*, allowing high-resolution, cross-sectional imaging of the anterior chamber angle and the ciliary body.[50] However, the typical 1310 nm wavelength light is blocked by pigment, preventing exploration behind the iris.[49]

Figure 8. Ultrasonic unit showing a section of an anterior eye

Ultrasonography

Ultrasonography uses high frequency mechanical pulses, usually generated by piezoelectric components, rather than light to assess the biometry of the anterior eye. The time for the reflected sound to return can be used to build up a picture of the front of the eye (Figure 8). A-scan along the optical axis allows assessment of corneal thickness, anterior chamber depth, lens thickness and axial length. B-scan ultrasonography scans across the eye, allowing a two-dimensional image of the ocular structures to be constructed. It has a precision of approximately 0.1 mm but only moderately high intra-observer and low inter-observer reproducibility.[51–53] It is an invasive technique and has reduced in popularity due to the commercialisation of a partial-coherent interferometric device for measuring axial length and calculating intraocular lens power. Partial-coherent interferometric measurements

of ocular axial length have a spatial resolution of approximately 0.01 mm and excellent reproducibility,[54] however, the latter technique cannot penetrate dense cataract as well as ultrasonography.[55] The resolution and depth of penetration of ultrasound are affected by transducer frequency. Traditional ultrasonography of the whole eye uses a 10 to 20 MHz transducer, with approximately 100 µm resolution achieving 25 mm penetration. High-frequency ultrasonic biomicroscopy (UBM) with a transducer of approximately 50 MHz increases the tissue resolution to 30 to 50 µm but reduces tissue penetration depth to four to five millimetres, which is still sufficient to image the anterior segment.[56,57] As the technique uses high frequency pulses rather than light waves, it can penetrate opaque corneas to examine the ciliary body and surrounding structures.

Computerised tomography

Computerised tomography (CT or CAT) emits several simultaneous X-rays from different angles. X-rays have high energy and a short wavelength and are able to pass through tissue. The beams, which are weaker if they have passed through dense tissue, are detected after they have passed through the body, creating a cross-sectional image. CT scans are far more detailed than ordinary X-rays. A liquid X-ray dye can be injected into the veins during the test to enhance organs, blood vessels or tumours. Far more X-rays are involved in a CT scan than in ordinary X-rays, increasing the potential side-effects and some patients experience side-effects due to allergic reactions to the liquid dye injected into the veins. For the eye, CT scans are usually used to assess ocular trauma, especially if a metal foreign body is suspected, in which case MRI is contraindicated.[58] However, CT may not differentiate whether the foreign body has penetrated the cornea and visibility will depend on the foreign body material.[59]

Magnetic resonance imaging

Magnetic resonance imaging (MRI) uses electro-magnetic waves combined with the reception of weak radio signals to record the density or concentration of hydrogen or other nuclei in the body.[8] MRI avoids health risks associated with ionising radiation found in routine X-rays and CT scans but can penetrate the whole human body. Furthermore, the resolution is greater than that of traditional CT scanning. The images of an MRI are reconstructed into cross-sections of anatomy (Figure 9). In ophthalmology, MRI has been used to examine the whole eye and orbit with respect to space occupying lesions, soft tissue damage and extra ocular muscle examination.[58,60,61] It has also been used to study eye shape with refractive error[62] and changes in the crystalline lens with accommodation.[63]

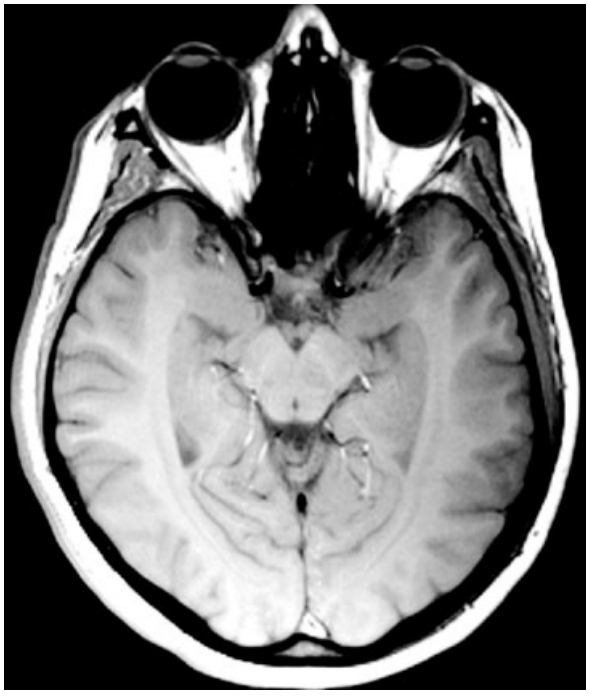

Figure 9. A head section across the ocular globes, obtained using a magnetic resonance imager

CONCLUSION

Imaging has advanced greatly over recent years with a combination of improved imaging chips and greater computer processing power. The digitally captured image can be visualised immediately and stored and retrieved easily. Images of the anterior eye, often using more than one technique, can assist in the detection, monitoring and documentation of disease, surgery and trauma. A better understanding of the physiology and topography of anterior ocular structures can also be achieved.

DECLARATION

The authors have no commercial or proprietary interest in any of the techniques mentioned in this review.

REFERENCES

1. Justice J Jr. Ophthalmic Photography. Boston: Little Brown and Company, 1982.
2. Jackman WT, Webster JD. On photographing the retina of the living human eye. *Philadelphia Photographer* 1886; 23: 275.
3. Coote J. The Illustrated History of Colour Photography, Fountain Press Ltd, 1993.
4. Tyler ME, Saine PJ, Bennett TJ. Practical Retinal Photography and Digital Imaging

Techniques. Boston: Butterworth Heineman, 2003.
5. Rosenfeld A. From image analysis to computer vision: An annotated bibliography, 1955–1979. *Comput Vis Image Underst* 2001; 84: 298–324.
6. Technical Advisory Service for Images (TASI): Advice paper on digital cameras. 2004 cited 2004 Jun 10. Available from: URL: http://www.tasi.ac.uk.
7. Charman WN. Imaging in the 21st Century. *Ophthalmic Physiol Opt* 1998; 18: 210–223.
8. Frame AJ, Undrill PE, Cree MJ, Olson JA, McHardy KC, Sharp PF, Forrester JV. A comparison of computer-based classification methods applied to the detection of microaneurysms in ophthalmic fluorescein angiograms. *Comput Biol Med* 1998; 28: 225–238.
9. Ege BM, Hejlesen OK, Larsen OV, Moller K, Jennings B, Kerr D, Cavan DA. Screening for diabetic retinopathy using computer based image analysis and statistical classification. *Comput Methods Programs Biomed* 2000; 62: 165–175.
10. Lim JI, LaBree L, Nichols T, Cardenas I. A comparison of digital non-mydriatic fundus imaging with standard 35-millimeter slides for diabetic retinopathy. *Ophthalmology* 2000; 107: 866–870.
11. Svedberg H, Chen E, Hamberg-Nystrom H. Changes in corneal thickness and curvature after different excimer laser photorefractive procedures and their impact on intraocular pressure measurements. *Graefes Arch Clin Exp Ophthalmol* 2005; 243: 1218–1220.
12. Cheng ACK, Fan D, Tang E, Lam DSC. Effect of corneal curvature and corneal thickness on the assessment of intraocular pressure using non-contact tonometry in patients after myopic LASIK surgery. *Cornea* 2006; 25: 26–28.
13. Megapixel.net Digital photography concepts cited 2004 Jun 21. Accessed from: URL: http://www.megapixel.net.
14. Taylor DJ, Jacob JS, Tooke JE. The integration of digital camera derived images with a computer based diabetes register for use in retinal screening. *Comput Methods Programs Biomed* 2000; 62: 157–163.
15. Basu A, Kamal AD, Illahi W, Khan M, Stavrou P, Ryder RE. Is digital image compression acceptable within diabetic retinopathy screening? *Diabet Med* 2003; 20: 766–771.
16. Yogesan K, Constable IJ, Eikelboom RH, van Saarloos PP. Tele-ophthalmic screening using digital imaging devices. *Aust NZ J Ophthalmol* 1998; 26 Suppl: S9–S11.
17. Newsom RS, Clover A, Costen MT, Sadler J, Newton J, Luff AJ, Canning CR. Effect of digital image compression on screening for diabetic retinopathy. *Br J Ophthalmol* 2001; 85: 799–802.
18. Kocsis O, Costaridou L, Mandellos G, Lymberopoulos D, Panayiotakis G. Compression assessment based on medical image quality concepts using computer-generated test images. *Comput Methods Programs Biomed* 2003; 71: 105–115.
19. Peterson RC, Wolffsohn JW. The effect of digital image resolution and compression on anterior eye imaging. *Br J Ophthalmol* 2005; 89: 828–830.
20. Wolffsohn J, Purslow C. Clinical monitoring of ocular physiology using digital image analysis. *Contact Lens Ant Eye* 2003; 26: 27–35.
21. Owen CG, Ellis TJ, Rudnicka AR, Woodward EG. Optimal green (red-free) digital imaging of conjunctival vasculature. *Ophthalmic Physiol Opt* 2002; 22: 234–243.
22. Polunin GS, Kourenkov VV, Polunina EG. Corneal transparency and measurement of corneal permeability in excimer laser photorefractive keratectomy. *J Refract Surg* 1998; 14 Suppl: S230–S234.
23. O'Donnell C, Wolffsohn JS. Grading of corneal transparency. *Contact Lens Ant Eye* 2004; 27: 161–170.
24. Friedman DS, Duncan DD, Munoz B, West SK, Schein OD. Digital image capture and automated analysis of posterior capsular opacification. *Invest Ophthalmol Vis Sci* 1999; 40: 1715–1726.
25. Lin A, Stern G. Correlation between pterygium size and induced corneal astigmatism. *Cornea* 1998; 17: 28–30.
26. Hockwin O, Lerman S, Ohrloff C. Investigations on lens transparency and its disturbances by microdensitometric analysis of Scheimpflug photographs. *Curr Eye Res* 1984; 3: 15–22.
27. Wegener A, Laser H. Image-analysis and Scheimpflug-photography in the anterior segment of the eye—a review article. *Klin Monatsbl Augenheilkd* 2001; 218: 67–77.
28. Dubbleman M, Van der Heijde GL, Weeber HA, Vrensen GFJM. Changes in the internal structure of the human crystalline lens with age and accommodation. *Vision Res* 2003; 43: 2363–2375.
29. Smith GTH, Brown NAP, Shun-shin GA. Light scatter from the central human cornea. *Eye* 1990; 4: 584–588.
30. Soya K, Amano S, Oshika T. Quantification of simulated corneal haze by measuring back-scattered light. *Ophthalmic Res* 2002; 34: 380–388.
31. van de Pol C, Soya K, Hwang DG. Objective assessment of transient corneal haze and its relation to visual performance after photorefractive keratectomy. *Am J Ophthalmol* 2001; 132: 204–210.
32. Morgan AJ, Harper J, Hosking SL, Gilmartin B. The effect of corneal thickness and corneal curvature on pneumatonometer measurements. *Curr Eye Res* 2002; 25: 107–112.
33. Koretz JF, Strenk SA, Strenk LM, Semmlow JL. Scheimpflug and high-resolution magnetic resonance imaging of the anterior segment: a comparative study. *J Opt Soc Am A—Opt Image Sci Vis* 2004; 21: 346–354.
34. Lackner B, Schmidinger G, Pieh S, Funovics MA, Skorpik C. Repeatability and reproducibility of central corneal thickness measurement with Pentacam, Orbscan and ultrasound. *Optom Vis Sci* 2005; 82: 892–899.
35. Hashemi H, Yazdani K, Mehravaran S, Fotouhi A. Anterior chamber depth measurement with A-scan ultrasonography, Orbscan II and IOLMaster. *Optom Vis Sci* 2005; 82: 900–904.
36. Liu Z, Huang AJ, Pflugfelder SC. Evaluation of corneal thickness and topography in normal eyes using the Orbscan corneal topography system. *Br J Ophthalmol* 1999; 83: 774–778.
37. Mejia-Barbosa Y, Malacara-Hernandez D. A review of methods for measuring corneal topography. *Optom Vis Sci* 2001; 87: 240–253.
38. Freegard TJ. The physical basis of transparency of the normal cornea. *Eye* 1997; 11: 465–471.
39. Bohnke M, Masters BR. Confocal microscopy of the cornea. *Prog Ret Eye Res* 1999; 18: 553–628.
40. Cavanagh HD, El-Agha MS, Petroll WM, Jester JV. Specular microscopy, confocal microscopy and ultrasound biomicroscopy —Diagnostic tools of the past quarter century. *Cornea* 2000; 19: 712–722.
41. Tervo T, Moilanen J. *In vivo* confocal microscopy for evaluation of wound healing following corneal refractive surgery. *Prog Ret Eye Res* 2003; 22: 339–358.
42. Popper M, Morgado AM, Quadrado MJ, Van Best JA. Corneal cell density measurement *in vivo* by scanning slit confocal microscopy: Method and validation. *Ophthalmic Res* 2004; 36: 270–276.
43. Moller-Pedersen T, Vogel M, Li HF, Petroll WM, Cavanagh HD, Jester JV. Quantification of stromal thinning, epithelial thickness, and corneal haze after photorefractive keratectomy using *in vivo* confocal microscopy. *Ophthalmology* 1997; 104: 360–368.
44. Reiser BJ, Ignacio TS, Wang YM, Taban M, Graff JM, Sweet P, Chen Z, Chuck RS. *In vitro* measurement of rabbit corneal epithelial thickness using ultrahigh resolution optical coherence tomography. *Vet Ophthalmol* 2005; 8: 85–88.
45. Hirano K, Ito Y, Suzuki T, Kojima T, Kachi S, Miyake Y. Optical coherence tomography for the noninvasive evaluation of the cornea. *Cornea* 2001; 20: 281–289.

46. King-Smith PE, Fink BA, Fogt N, Nichols KK, Hill RM, Wilson GS. The thickness of the human precorneal tear film: evidence from reflection spectra. *Invest Ophthalmol Vis Sci* 2000; 41: 3348–3359.
47. Wang J, Fonn D, Simpson TL, Jones L. Precorneal and pre- and post-lens tear film thickness measured indirectly with optical coherence tomography. *Invest Ophthalmol Vis Sci* 2003; 44: 2524–2528.
48. Feng YW, Simpson TL. Comparison of human central cornea and limbus *in vivo* using optical coherence tomography. *Optom Vis Sci* 2005; 82: 416–419.
49. Baikoff G, Lutun E, Ferraz C, Wei J. [Analysis of the eye's anterior segment with optical coherence tomography. Static and dynamic study]. *J Fr Ophtalmol* 2005; 28: 343–352.
50. Hoerauf H, Scholz C, Koch P, Engelhardt R, Laqua H, Birngruber R. Trans-scleral optical coherence tomography—A new imaging method for the anterior segment of the eye. *Arch Ophthalmol* 2002; 120: 816–819.
51. Urbak SF. Ultrasound biomicroscopy. I. Precision of measurements. *Acta Ophthalmol Scand* 1998; 76: 447–455.
52. Urbak SF. Ultrasound biomicroscopy. III. Accuracy and agreement of measurements. *Acta Ophthalmol Scand* 1999; 77: 293–297.
53. Urbak SF, Pedersen JK, Thorsen TT. Ultrasound biomicroscopy. II. Intraobserver and interobserver reproducibility of measurements. *Acta Ophthalmol Scand* 1998; 76: 546–549.
54. Santodomingo-Rubido J, Mallen EAH, Gilmartin B, Wolffsohn JS. A new non-contact optical device for ocular biometry. *Br J Ophthalmol* 2002; 86: 458–462.
55. Freeman G, Pesudovs K. The impact of cataract severity on measurement acquisition with the IOLMaster. *Acta Ophthalmol Scand* 2005; 83: 439–442.
56. Pavlin CJ, Sherar MD, Foster FS. Subsurface ultrasound microscopic imaging of the intact eye. *Ophthalmology* 1990; 97: 244–250.
57. Pavline CJ, Harasiewicz K, Foster FS. Ultrasound biomicroscopy of anterior segment structures in normal and glaucomatous eyes. *Am J Ophthalmol* 1992; 113: 381–389.
58. Kolk A, Pautke C, Wiener E, Ploder O, Neff A. A novel high-resolution magnetic resonance imaging microscopy coil as an alternative to the multislice computed tomography in postoperative imaging of orbital fractures and computer-based volume measurement. *J Oral Maxilofacial Surg* 2005; 63: 492–498.
59. Deramo VA, Shah GK, Baumal CR, Fineman MS, Correa ZM, Benson WE, Rapuano CJ, Cohen EJ, Augsburger JJ. The role of ultrasound biomicroscopy in ocular trauma. *Tr Am Ophthalmol Soc* 1998; 96: 355–365.
60. Ben Simon GJ, Annunziata CC, Fink J, Villablanca P, McCann JD, Goldberg RA. Rethinking orbital imaging—Establishing guidelines for interpreting orbital imaging studies and evaluating their predictive value in patients with orbital tumors. *Ophthalmology* 2005; 112: 2196–2207.
61. Sa HS, Kyung SE, Oh SY. Extraocular muscle imaging in complex strabismus *Ophthalmic Surg Lasers Imaging* 2005; 36: 487–493.
62. Atchison DA, Jones CE, Schmid KL, Pritchard N, Pope JM, Strugnell WE, Riley RA. Eye shape in emmetropia and myopia. *Invest Ophthalmol Vis Sci* 2004; 45: 3380–3386.
63. Jones CE, Atchison DA, Meder R, Pope JM. Refractive index distribution and optical properties of the isolated human lens measured using magnetic resonance imaging (MRI). *Vision Res* 2005; 45: 2352–2366.

Corresponding author:
Dr James Wolffsohn
Ophthalmic Research Group
School of Life and Health Sciences
Aston University, Aston Triangle
Birmingham, B4 7ET
UNITED KINGDOM
E-mail: j.s.w.wolffsohn@aston.ac.uk